AN IMPROVED LOCAL BINARY PATTERN OPERATOR FOR TEXTURE CLASSIFICATION

Fuxiang Lu[*]

School of Information Science & Engineering
Lanzhou University
222 Tianshui Road, Lanzhou, 730000, China

Jun Huang[†]

Shanghai Advanced Research Institute
Chinese Academy of Sciences
99 Haike Road, Shanghai, 201210, China

ABSTRACT

Based on pattern uniformity measure and the number of ones in the Local Binary Pattern (LBP) codes, this paper proposes an Improved Local Binary Pattern (ILBP) operator to describe local image texture more effectively. The ILBP operator discovers an important group of basic primitives such as lines, T-junctions, and cross-intersections, which are ignored by uniform LBP operator. Such local primitives are as crucial as those represented by uniform patterns for recognition tasks. The resulting ILBP feature is more discriminative than traditional LBP feature although they are both invariant in terms of monotonic gray-scale variation and rotation transformation.

***Index Terms*—** Texture classification, local binary pattern, rotation invariance

1. INTRODUCTION

Natural surfaces generally exhibit some repetitive gray-scale variations or patterns which are usually referred to as texture. Texture classification plays a significant role in pattern recognition and computer vision applications such as object recognition, medicine image analysis, material surface inspection, image retrieval, and etc [1].

Early works focus on statistical analysis of texture images such as the co-occurrence matrix method [2]. Later, model-based methods, e.g. Gaussian Markov Random Fields (GMRF) [3] were introduced. Furthermore, signal processing methods such as Gabor filtering [4] and discrete wavelet transform [5], provide efficient multi-resolution tools for analyzing textures. These techniques can achieve impressive classification results on data sets collected under relatively well controlled conditions. However, many of the above methods are sensitive to geometric and photometric transformations.

In [6], Ojala et al. proposed a gray-scale and rotation invariant feature by observing the statistical distributions of uniform Local Binary Patterns (LBPs). LBP is a simple yet efficient operator to describe local image pattern. Uniform patterns occur more frequently than others, and they have a limited number of bitwise transitions in the circular binary representation. In uniform LBP mapping, every uniform pattern is assigned to a separate label and all others are collected into a single label. The local primitives represented by uniform patterns consist of spots, edges, corners, and flat regions. To achieve rotation invariance, each uniform binary pattern can be circularly rotated to its minimum value.

As the size of circular neighborhood increases, non-uniform patterns account for more and more percent of all patterns. For example, when the $(8,1)$, $(16,2)$, and $(24,3)$ neighborhoods are used, non-uniform patterns contribute 12.8%, 33.1%, and 50.7%, respectively [6]. Merging all non-uniform patterns under the same "miscellaneous" label unavoidably leads to much information loss. To tackle this issue, this paper proposes an Improved Local Binary Pattern (ILBP) operator based on pattern uniformity measure and the number of ones in the LBP codes. In the case of ILBP, information in non-uniform patterns is extracted and also used for texture classification.

Comparing with uniform LBP, the ILBP operator succeeds in discovering an important group of basic primitives such as lines, T-junctions, and cross-intersections, which are ignored by uniform LBP operator. Although such primitives may not occur as frequently as those represented by uniform patterns, they are also crucial for recognition tasks. Thus, the ILBP feature is more discriminative than uniform LBP feature. This will be attested by experimental results on texture data sets in Section 3. The ILBP feature is also invariant in terms of monotonic gray-scale variation, rotation transformation, and histogram equalization processing. Finally, the ILBP operator is computationally attractive because it can be realized with a few operations and a look-up table.

2. IMPROVED LOCAL BINARY PATTERN

2.1. Local binary pattern

Given a pixel with coordinates (x, y), let us first define its neighborhood, denoted by (P, R), as a set of P sampling points on a circle of radius R around pixel (x, y). These sam-

[*]Thanks to the Basic Scientific Research Business Expenses of the Central University, Open Project of Key Laboratory for Magnetism and Magnetic Materials of the Ministry of Education, Lanzhou University (LZUMMM2015010), and NSFC (61201422) for funding.

[†]Thanks to NSFC (61201446) and the National Key Technology R&D Program (2012BAH43F03) for funding.

pling points around pixel (x,y) lie at coordinates

$$(x_p, y_p) = (x + R\cos(2\pi p/P),\, y - R\sin(2\pi p/P)).$$

Now, the LBP code for the center pixel (x,y) is defined as follows [6, 7]:

$$LBP_{P,R} = \sum_{p=0}^{P-1} s(g_p - g_c)2^p, \tag{1}$$

$$s(z) = \begin{cases} 1, & \text{if } z \geq 0, \\ 0, & \text{otherwise}, \end{cases} \tag{2}$$

where g_c is the intensity value of the center pixel (x,y), and g_p is the intensity value of the p-th neighbor. When a neighbor does not fall at integer coordinates, its intensity value is determined by bilinear interpolation.

After the LBP code of each pixel (except pixels on the boundary) in an image of size $M \times N$ is computed, a 2^P-bin histogram of such LBP codes is commonly used for further analysis of the image

$$h(k) = \sum_{x=1}^{M-2}\sum_{y=1}^{N-2} \delta(LBP_{P,R}(x,y), k), k \in [0, 2^P - 1], \tag{3}$$

where $\delta(u,v)$ is Kronecker delta function and

$$\delta(u,v) = \begin{cases} 1, & \text{if } u = v, \\ 0, & \text{otherwise}. \end{cases}$$

An extension to the original LBP operator is the so-called uniform LBP, denoted here as $LBP^{u2}_{P,R}$. The uniformity measure of an LBP pattern is defined as the number of bitwise transitions in that pattern

$$U(LBP_{P,R}) = \sum_{p=0}^{P-1} \left| s(g_{p+1} - g_c) - s(g_p - g_c) \right|, \tag{4}$$

where g_P is equivalent to g_0. An LBP is called uniform if $U(LBP_{P,R}) \leq 2$. In the computation of the $LBP^{u2}_{P,R}$ histogram, uniform patterns are used so that the histogram has a separate bin for every uniform pattern and all non-uniform patterns are accumulated into a single bin. As such, the number of patterns is reduced from 2^P to $P(P-1)+3$. For example, $LBP_{8,1}$ consists of 256 patterns whereas $LBP^{u2}_{8,1}$ has only 59 patterns.

The original rotation invariant LBP operator based on uniform patterns, denoted here as $LBP^{riu2}_{P,R}$, is defined as

$$LBP^{riu2}_{P,R} = \begin{cases} \sum\limits_{p=0}^{P-1} s(g_p - g_c), & \text{if } U(LBP_{P,R}) \leq 2, \\ P+1, & \text{otherwise}. \end{cases} \tag{5}$$

An example of applying $LBP_{8,1}$, $LBP^{u2}_{8,1}$, and $LBP^{riu2}_{8,1}$ to a 3×3 image block is illustrated in (6), where for simplicity the center pixel is compared with its immediate 8-neighbors. The eight bits obtained from intensity comparisons can be collected in any order (we put together them clockwise, starting from the uppermost, leftmost bit). Note that in this example "11100010" is a non-uniform pattern as $U = 4$, so it is labeled 58 (i.e. $P(P-1)+2$) for $LBP^{u2}_{8,1}$ and 9 (i.e. $P+1$) for $LBP^{riu2}_{8,1}$.

$$\begin{array}{|c|c|c|}\hline 64 & 32 & 48 \\ \hline 16 & 32 & 16 \\ \hline 48 & 16 & 8 \\ \hline \end{array} \Rightarrow \underset{(11100010)_2}{\begin{array}{|c|c|c|}\hline 1 & 1 & 1 \\ \hline 0 & \cdot & 0 \\ \hline 1 & 0 & 0 \\ \hline \end{array}} \Rightarrow \begin{cases} LBP_{8,1} = 226, \\ LBP^{u2}_{8,1} = 58, \\ LBP^{riu2}_{8,1} = 9. \end{cases} \tag{6}$$

2.2. Improved local binary pattern

As mentioned in Section 1, non-uniform patterns account for more and more percent of all patterns as the size of the involved neighborhood increases. For example, Ojala et al. has noticed that above 50% of all patterns are non-uniform for natural texture images when the $(24,3)$ neighborhood is used in tradition LBP operator [6]. It is worth pointing out that some of such non-uniform patterns are indeed statistically insignificant, and hence noise-prone and unreliable. In contrast, the rest of such non-uniform patterns are statistically significant and their occurrence probabilities can be estimated reliably. Thus, accumulating all non-uniform patterns into a single bin discards a large amount of texture information.

Analyzing local binary pattern obtained by the LBP operator, we find that a bitwise transition from 0 to 1 in the circular representation of the pattern always accompanies a bitwise transition from 1 to 0 and vice versa. Since the uniformity value $U(LBP_{P,R})$, as defined in (4), corresponds to the number of spatial transitions in the pattern, it can only take an even number between 0 to P. Another observation is that some non-uniform patterns with $U(LBP_{P,R}) > 2$ also represent an important group of basic primitives, e.g. lines, T-junctions, and cross intersections, as shown in Fig. 1. Evidently, such primitives are crucial for recognition tasks.

In order to extract information in all patterns, and meanwhile keep the resulting feature vector compact, we propose an improved local binary pattern operator, denoted here as $ILBP_{P,R}$. It assigns every uniform pattern to a separate label, ranging from 0 to $P(P-1)+1$. In other words, the ILBP code is equivalent to the LBP code if it is uniform. However, comparing with $LBP^{u2}_{P,R}$, the treatment of non-uniform patters is totally different for $ILBP_{P,R}$. For $LBP^{u2}_{P,R}$, all non-uniform patterns are assigned to a "miscellaneous" label, whereas for $ILBP_{P,R}$, non-uniform patterns with a fixed uniformity value are given a separate label. Consequently, $ILBP_{P,R}$ has $P^2 - \frac{P}{2} + 1$ (i.e. $P(P-1)+2$ plus $\frac{P}{2} - 1$) distinct output values in total.

To achieve rotation invariance, a locally rotation invariant

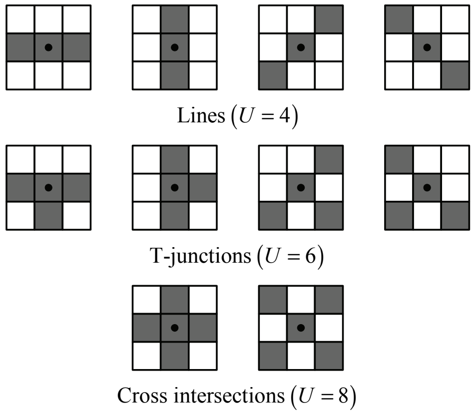

Fig. 1. Some basic primitives detected by $ILBP_{8,1}^{ri}$. White and gray rectangles correspond to bit values of 0 and 1 in binary patterns.

ILBP can be defined as

$$ILBP_{P,R}^{ri} = \begin{cases} \sum_{p=0}^{P-1} s(g_p - g_c), & \text{if } U(LBP_{P,R}) \leq 2, \\ P - 1 + \frac{U}{2}, & \text{otherwise}, \end{cases} \tag{7}$$

where U is defined in (4). By doing so, the $ILBP_{P,R}^{ri}$ operator has $\frac{3}{2}P$ distinct output labels. In practice, the mapping from $LBP_{P,R}$ to $ILBP_{P,R}$ or $ILBP_{P,R}^{ri}$ can be implemented with a lookup table of 2^P elements, and then the histogram of $ILBP_{P,R}$ or $ILBP_{P,R}^{ri}$ can be easily obtained.

3. EXPERIMENTAL RESULTS

We evaluate the performance of the proposed ILBP operator on two texture data sets: RotInv_16_10 [6] and Outex [6]. For both data sets, we use the Nearest Neighbor (NN) classifier with G-statistic [8] distance measure, as defined in (8).

$$D(\mathbf{s}, \mathrm{m}) = -\sum_{b=1}^{B} s_b \log(m_b + s_b), \tag{8}$$

where $\mathbf{s}$ and $\mathbf{m}$ are the ILBP histograms for the testing and training samples; B is the number of bins; s_b and m_b are two sample probabilities at bin b. A testing sample is assigned to the class of the training sample with minimum G-statistic distance.

3.1. Experiments on RotInv_16_10

The RotInv_16_10 data set is previously utilized to conduct rotation invariant texture classification in [6]. Textures are presented at 10 different rotation angles (0°, 20°, 30°, 45°, 60°, 70°, 90°, 120°, 135°, and 150°). For each class, there are 1210 16×16 training samples and 70 180×180 testing samples, with 121 training samples and 7 testing samples per angle. Hence, there are a total of 20480 $((1210 + 70) \times 16)$ samples in RotInv_16_10. It should be stressed that such small size of training samples increases the difficulty of texture classification significantly. Fig 2 shows some testing samples from RotInv_16_10, with one image per class.

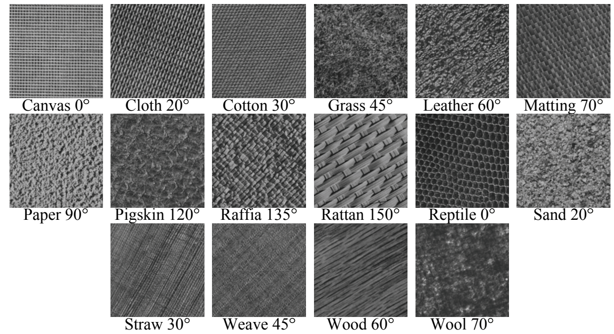

Fig. 2. Samples from RotInv_16_10 at particular angles.

Table 1. Classification accuracies (%) on RotInv_16_10.

Training angle	$LBP_{P,R}^{riu2}$ (8,1)	(16,2)	(24,3)	$ILBP_{P,R}^{ri}$ (8,1)	(16,2)	(24,3)
0°	68.2	96.2	98.7	67.8	97.6	97.6
20°	86.1	99.0	98.9	86.3	99.9	99.9
30°	84.7	98.7	99.1	85.3	99.7	99.4
45°	76.1	99.1	97.6	76.6	99.6	99.4
60°	84.7	98.3	99.2	85.0	98.4	98.6
70°	84.2	99.1	98.2	84.6	99.7	98.2
90°	69.3	97.6	100.0	68.1	97.8	99.5
120°	84.4	98.6	98.6	85.4	99.5	99.4
135°	76.0	98.6	96.7	76.2	98.9	97.5
150°	84.4	97.7	98.0	85.0	98.8	99.2
Mean	79.8	98.3	98.5	**80.0**	**99.0**	**98.9**

We adopt the same experimental setup as that in [6]. The experiments are repeated ten times. For each run, the 16×16 samples of just one rotation angle are used as training data and the samples of the other nine rotation angles are used as testing data. Hence, in this case, we have 1936 16×16 training samples and 1008 180×180 testing samples.

Table 1 shows classification accuracy rates on RotInv_16_10. We observe from Table 1 that the average performance improvement of $ILBP_{P,R}^{ri}$ over $LBP_{P,R}^{riu2}$ is 0.2%, 0.7%, and 0.4% respectively when (P, R) is $(8, 1)$, $(16, 2)$, and $(24, 3)$. Since the classifier is trained with samples of just one rotation angle, this setup is a true test for different LBP operators' ability to produce a rotation invariant description of local region. Thus, experimental results on RotInv_16_10 show that $ILBP_{P,R}^{ri}$ is more discriminative than $LBP_{P,R}^{riu2}$ although they are both invariant to rotation transformation.

3.2. Experiments on Outex

The Outex data set [6] is comprised of textural images from a wide variety of real materials. Outex also provides some ready-made test suits to evaluate algorithms for various types of texture analysis. In our experiments, we use two test suits: Outex_TC_00010 (TC10) and Outex_TC_00012 (TC12), which are created for rotation invariant texture classification, and rotation & illumination invariant texture classification, respectively.

The same 24 classes of textures are contained in TC10 and TC12, where each texture is captured using 3 different illuminations ("horizon", "inca", and "tl84") and 9 different rotation angles ($0°$, $5°$, $10°$, $15°$, $30°$, $45°$, $60°$, $75°$ and $90°$). For each of 24 textures, we have 20 128×128 samples for each illumination and rotation angle. The experimental setups for TC10 and TC12 are as follows:

- TC10: 20 samples in each texture class with illumination "inca" and $0°$ angle are served as training data, and 160 samples in each class with the same illumination but the other 8 rotation angles are reserved as testing data. Hence, there are 480 (24×20) training samples and 3840 ($24 \times 8 \times 20$) testing samples in total.
- TC12: The classifiers are trained with the same training samples as TC10 but tested twice with all samples captured using the other two illumination conditions: "tl84" (problem 000) and "horizon" (problem 001). Therefore, there are a total of 480 (24×20) training samples and 4320 ($24 \times 9 \times 20$) testing samples in both problems.

Table 2 shows the classification results of $LBP_{P,R}^{riu2}$ and $ILBP_{P,R}^{ri}$ on TC10 and TC12, respectively. From Table 2, we can make the following findings.

First, $ILBP_{P,R}^{ri}$ always outperforms $LBP_{P,R}^{riu2}$ on both test suits. It is in accordance with our analysis in Section 2.2 that $ILBP_{P,R}^{ri}$ has more discriminative ability than $LBP_{P,R}^{riu2}$. For example, above 1% improvement is obtained on TC10 regardless of the values of (P, R). The largest gain on TC12 is 3.1%, obtained when $(P, R) = (16, 2)$ and the samples with 'horizon' illumination condition are used as testing data.

Second, the accuracy rates deteriorate clearly when the illumination conditions used for capturing training and testing samples are different. For example, the performance of $ILBP_{16,2}^{ri}$ drops from 91.7% to 78.7% if we change the illumination used for testing data from 'inca' to 'horizon'. This validates that changing illumination conditions significantly increases the difficulty of texture classification and thus the TC12 setup is more challenging than TC10.

Table 2. Classification accuracies (%) on TC10 and TC12.

	$LBP_{P,R}^{riu2}$			$ILBP_{P,R}^{ri}$		
(P, R)	TC10	TC12		TC10	TC12	
		'tl84'	'horizon'		'tl84'	'horizon'
$(8, 1)$	84.2	65.0	63.7	**85.4**	**66.4**	**65.1**
$(16, 2)$	89.4	82.4	75.6	**91.7**	**83.5**	**78.7**
$(24, 3)$	95.3	85.2	81.3	**96.3**	**86.3**	81.3

4. CONCLUSION

By analyzing the weakness of uniform LBP operator, this paper proposes an ILBP operator based on pattern uniformity measure and the number of ones in the LBP codes. ILBP is invariant in terms of monotonic gray-scale change, histogram equalization operation, and rotation transformation. A major advantage of ILBP over traditional LBP is that it detects a large group of local primitives from non-uniform patterns. Therefore, the ILBP feature makes a better tradeoff between the discriminative ability and robustness. Finally, ILBP is computationally attractive and well suited for real-world applications because it can be realized with a few operators and a look-up table.

5. REFERENCES

[1] M. Mirmehdi, X. Xie, and J. Suri, Eds., *Handbook of Texture Analysis*, Imperial College Press, London, 2008.

[2] R.M. Haralick, K. Shanmugam, and I. Dinstein, "Textural features for image classification," *IEEE Trans. Syst. Man. Cybern.*, vol. 3, no. 6, pp. 610–621, Nov. 1973.

[3] R. Chellappa and S. Chatterjee, "Classification of textures using Gaussian Markov random fields," *IEEE Trans. Acoust., Speech, Signal Process.*, vol. 33, no. 4, pp. 959–963, Aug. 1985.

[4] A.C. Bovik, M. Clark, and W.S. Geisler, "Multichannel texture analysis using localized spatial filters," *IEEE Trans. pattern Anal. Mach. Intell.*, vol. 12, no. 1, pp. 55–73, Jan. 1990.

[5] G. Van de Wouwer, P. Scheunders, and D. Van Dyck, "Statistical texture characterization from discrete wavelet representations," *IEEE Trans. Image Process.*, vol. 8, no. 4, pp. 592–598, Apr. 1999.

[6] T. Ojala, M. Pietikäinen, and T. Mäenpää, "Multiresolution gray-scale and rotation invariant texture classification with local binary patterns," *IEEE Trans. Pattern Anal. Mach. Intell.*, vol. 24, no. 7, pp. 971–987, Jul. 2002.

[7] M. Pietikäinen, A. Hadid, G. Zhao, and T. Ahonen, *Computer Vision Using Local Binary Patterns*, Springer-Verlag London Limited, London, 2011.

[8] J. Ren, X. Jiang, and J. Yuan, "Noise-resistant local binary pattern with an embedded error-correction mechanism," *IEEE Trans. Image Process.*, vol. 22, no. 10, pp. 4049–4060, Oct. 2013.